Original paper

3D-printed template and optical needle navigation in CT-guided iodine-125 permanent seed implantation

Zhe Ji, MD, Yuliang Jiang, MB, Haitao Sun, MB, Yi Chen, MD, Fuxin Guo, MD, Jinghong Fan, MB, Junjie Wang, MD, PhD

Department of Radiation Oncology, Peking University Third Hospital, Beijing, China

Abstract

Purpose: To preliminarily verify the accuracy of navigation-assisted seed implantation by comparing pre-operative and actual differences in puncture characteristics and dosimetry in computed tomography (CT)-guided, navigation-assisted radioactive iodine-125 seed implantation, using 3D-printed templates for malignant tumors' treatment.

Material and methods: A total of 27 tumor patients, who were treated with seed implantation under combination guidance in our hospital between December 2019 and December 2020 were enrolled in this study. Navigation needles (n = 1-3) were placed in each patient to obtain pre-operative and intra-operative puncture information, such as angle, depth, insertion point, and tip position. Moreover, dosimetry parameters in pre-operative and post-operative plans, including D_{90}, V_{100}, V_{150}, V_{200}, minimum peripheral dose (MPD), conformal index, external index, and homogeneity index of target area were investigated.

Results: Mean errors of the angle, depth, insertion point, and tip position were 0.5 ±0.5°, 4.0 ±2.0 mm, 1.7 ±1 mm, and 3.1 ±1.8 mm, respectively. There were no significant differences between intra-operative and pre-operative angles (p = 0.271), but there was a significant difference in the depth (p = 0.002). Errors of the angle, depth, and insertion point were larger for the pelvic/retroperitoneal area than for the head and neck/chest wall ($p < 0.05$). With the exception of MPD, there was no significant difference in dosimetry indices between post-operative and preoperative plans ($p > 0.05$).

Conclusions: Seed implantation under combination guidance showed good accuracy, and the actual intra-operative puncture information and post-operative doses were in agreement with those in the pre-operative plan, thereby demonstrating promising prospects for further development.

J Contemp Brachytherapy 2021; 13, 4: 410–418
DOI: https://doi.org/10.5114/jcb.2021.108595

Key words: brachytherapy, iodine-125, optical navigation, 3D-printed template, accuracy.

Purpose

Radioactive iodine-125 (^{125}I) seed implantation is being increasingly used for local treatment of tumors [1]. However, as the puncture procedure largely depends on a physician's clinical experience and level of expertise, quality of the procedure and treatment effect vary, limiting promotion of radioactive ^{125}I seed implantation for clinical use. Three-dimensional (3D)-printed template technology is a milestone in the advancement of radioactive ^{125}I seed implantation therapy. With 3D-printed template guidance, accurate control of the seed needle has been realized, greatly improving adherence to pre-operative plan [2, 3]. Recently, various studies have used an image navigation system to assist in the treatment of head and neck tumors using seed implantation, achieving good puncture accuracy [4]. This study applied an image navigation system and 3D-printed template to radioactive ^{125}I seed implantation treatment for tumors in different parts of the body to evaluate puncture and dose accuracy, and provide a theoretical basis and data support for rational selection and optimization of implantation protocols.

Material and methods

Baseline clinical data

A total of 27 patients with malignant tumors, who presented in our department between December 2019 and December 2020 were enrolled in this study. They were treated using an image navigation system, 3D-printed templates, and computed tomography (CT) to guide radioactive ^{125}I seed implantation. All patients had complete imaging data, pre-operative/post-operative plans, and intra-operative data. All patients had been discussed in a multidisciplinary tumor board before receiving treat-

Address for correspondence: Junjie Wang, MD, PhD, Department of Radiation Oncology, Peking University Third Hospital, 49th North Garden Road, Haidian District Beijing, China, Zip: 100191, ✉ e-mail: junjiewang_edu@sina.cn; aschoff@126.com

Received: 28.04.2021
Accepted: 15.06.2021
Published: 24.08.2021

ment, and met the criteria for radioactive seed implantation [1]: 1) patients who showed relapse after surgery or external radiotherapy or refused surgery or external radiotherapy with a tumor diameter ≤ 7 cm, 2) clear pathological diagnosis, 3) a suitable puncture path, 4) no bleeding tendency or hypercoagulable state, 5) good general physical condition (Karnofsky performance status score > 70), so that radioactive seed implantation could be tolerated, and 6) expected survival > 3 months. All patients signed an informed consent prior to treatment. The research protocol was approved by an ethics committee.

Information on systems, materials, and equipment

Brachytherapy treatment planning system KLSIRPS-3D, Beijing University of Aeronautics and Astronautics, and Beijing Astro Technology was used. The source data in the planning system were derived from TG 43 and its updated document issued by the American Association of Physicists in Medicine [5, 6]. Philips' Brilliance Big Bore CT scanner, and IGS-MO Optical Image Navigation system and Xinbo Medical Technology (Figure 1) were applied. 3D templates were produced from 3D photocuring rapid-prototyping machine printing (Shanghai 3D Union Tech, RS6000) with an accuracy of 0.1 mm, and photocurable resins that comply with the European Communities standards were used as printing materials. ^{125}I seeds, type 6711_1985 (HTA Co., Ltd., China) with a half-life of 59.4 days and dose-rate constant of 0.965 cGy/(h·U) were utilized. For radioactive ^{125}I seed implantation, Mick Radio-Nuclear Instruments and Eckert & Ziegler BEBIG devices were used.

Pre-operative plan

3D template-guided radioactive ^{125}I seed implantation in accordance with the previous research and published professional standards [7, 8] was performed. Image navigation system assistance was applied based on the following aspects:

1. Positioning and pre-operative plan design:
   A. CT, with a slice thickness of 2.5 mm was performed 2 days before the operation. The position (supine/prone/lateral) was selected according to the location of lesion; the vacuum pad was fixed, and the body surface was marked with a pendulum line.
   B. CT data were transmitted to brachytherapy treatment planning system to develop a pre-operative plan design. The tumor in target area (gross tumor volume – GTV) and organs at risk (OARs) within 2 cm around the target area were outlined to set the prescribed dose and seed activity as well as to identify the direction, distribution, and depth of the seed needle and set up 1-3 seed needles as navigation needles. The number of seeds was calculated

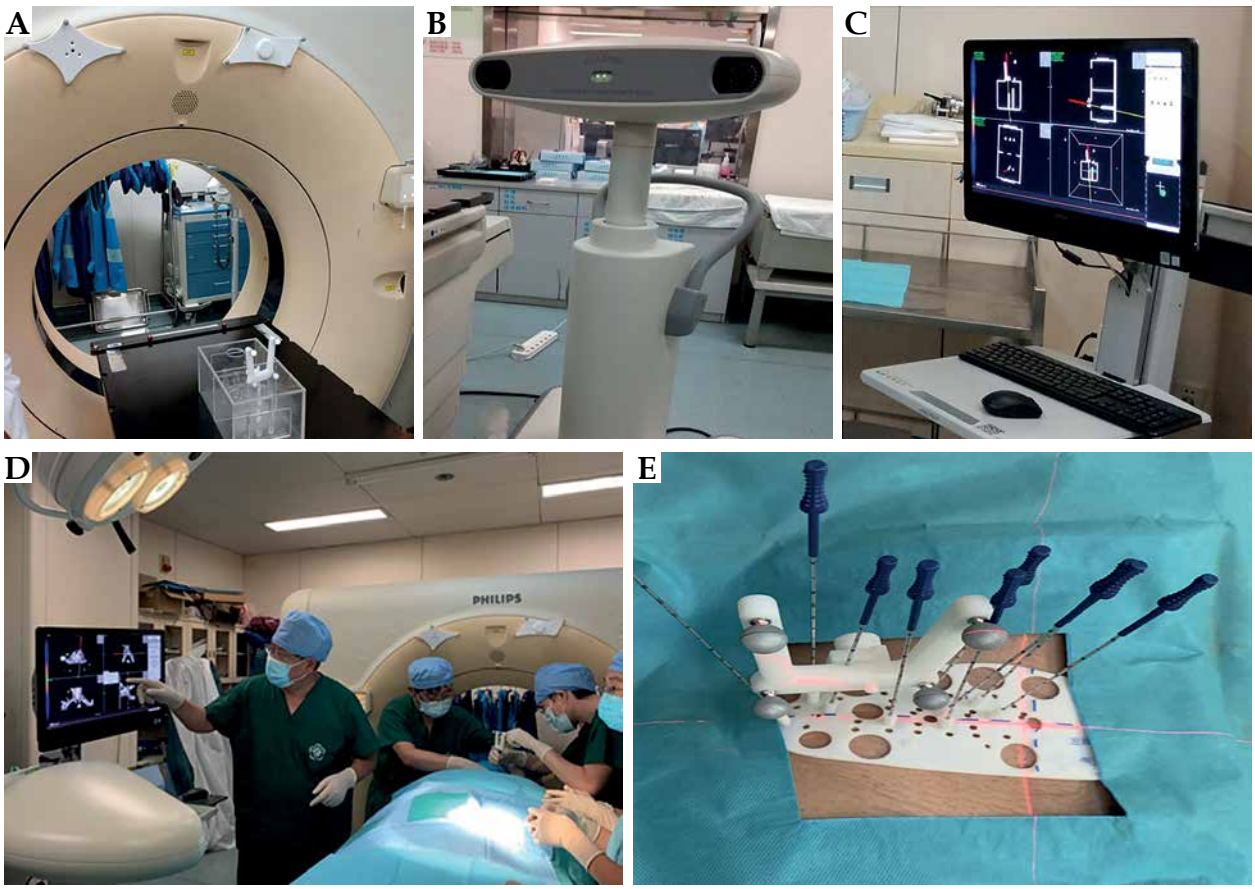

Fig. 1. Image navigation system composition. **A**) CT locator and optical tracer for needle position; **B**) Optical sensing device; **C**) Image registration and real-time display system; **D, E**) Real-time operator-guided surgery

and spatial distribution of the seeds was simulated. The design of needle path should follow principles such as: staying within a space of 1 cm, trying to keep parallel arrangement at the same layer, protecting and avoiding important structures, including nerves, large blood vessels, and cavity viscera, and trying to avoid any bones on the puncture path. Based on these, the number of needles should be as little as possible. Seed activity was usually 0.4-0.6 mCi, and seed spacing design was within 0.5-1.0 cm (which may vary with seed activity and prescription dose) and at least 0.5 cm away from OARs. Using computer optimization combined with manual adjustment, GTV D_{90} (minimum dose to 90% of the volume of GTV) was adjusted to meet the prescribed dose setting requirements. At the same time, the maximum dose of OARs should not exceed the prescribed dose, and the dose of OARs should be as low as possible.

2. Design and production of 3D templates:
   A. Personalized digital modeling of the treatment area template in brachytherapy treatment planning system, and additional information on alignment axis and puncture characteristics were used to set the printing range of template.
   B. A 3D template was printed using a 3D photocuring rapid-prototyping machine and medical photocuring resin material. The 3D templates included body surface information, alignment marks, and puncture information with respect to the patients' treatment area. The thickness of the template was 2.5 mm, and the length of the guide hole was 13 mm. Therefore, the total thickness of the part with the guide hole was 15.5 mm, which ensured that the needle insertion was accurately directed. The diameter of the seed needles was 1.27 ±0.01 mm, and the inner wall of the template guide hole was 1.4 mm in diameter, which ensured smooth insertion of the needle and no movement in the guide hole.
3. Patient reset and image navigation system-assisted 3D-printed template alignment and fixation:
   A. The patient was reset with reference to the positioning mark, and the template was aligned as per the positioning mark, template's coordinates, and contour of the patient's body surface.
   B. An optical tracer was placed on CT frame and 1-3 seed needles (navigation needles), so the relative positions of CT, navigation needle, and patient were confirmed. CT was performed with the image information transmitted to the image navigation system, and the virtual navigation needle could be seen on the patient's CT images in the image navigation system (in an ideal state, the position of the virtual navigation needle in the patient's image should be consistent with the position of actual navigation needle). Then, the navigation needle was inserted under the guidance of virtual navigation needle.
   C. After the insertion of navigation needle was completed, CT was performed to confirm accuracy of the needles' position, and fine-tuning was conducted if there was an error. After the navigation needles were correctly calibrated, the 3D template's position was considered accurate.
4. Puncture and seed implantation:
   A. After the 3D template was accurately positioned, the rest of seed needles were percutaneously punctured to the predetermined depth through a template guide hole. During the puncture process, CT was performed to monitor the needle insertion path and depth, and the needle was fine-tuned, if necessary, to avoid damage to organs at risk.
   B. After all the needles were in place, the seeds were implanted one by one according to pre-operative plan, and CT was performed to confirm seed distribution.
   C. As there could be differences between the actual intra-operative situation and pre-operative plan, intra-operative optimization was carried out, if necessary, and the needle insertion path and seed distribution were adjusted in real-time to ensure that the dose received by GTV met the requirements of pre-operative plan.
5. Post-operative dose evaluation: CT was performed post-operatively; the image was transmitted to the brachytherapy treatment planning system, the target area was recontoured on a final CT for dose verification, and the actual doses delivered to GTV and organs at risk were evaluated. Technical process is presented in Figure 2. The post-operative dose quality evaluation complied with the quality evaluation standard defined by the BC Cancer Research Center [9]. According to immediate verification of target areas D_{90} and V_{100} (volume when GTV receives 100% of the prescribed dose), the evaluation results were characterized as excellent, good, fair, and poor (excellent: $V_{100} \geq 90\%$, $125\% \geq D_{90} \geq 100\%$ [prescription dose]; good: $90\% > V_{100} > 85\%$, $100\% > D_{90} > 90\%$; fair: $85\% \geq V_{100} \geq 75\%$, $90\% \geq D_{90} \geq 80\%$, or $D_{90} > 125\%$; poor: $V_{100} < 75\%$, $D_{90} < 80\%$).

Collection and comparison of treatment parameters

Puncture information: In the brachytherapy treatment planning system, the images registered after placing intra-operative navigation needles were fused with pre-operative plan images, and rigid registration for the bone was performed. In the fusion image, both the preplanned and actual puncture characteristics were displayed. The angle and depth of the puncture before and during the procedure were compared, and the absolute value of difference was taken as the error value. Meanwhile, straight-line distances between two punctures' points on the body surface and between two tips' positions were recorded.

Dosimetry information: In the brachytherapy treatment planning system, every dosimetry parameter from pre-operative and post-operative plans was recorded and compared, including GTV D_{90}, V_{100}, V_{150} (volume when GTV receives 150% of the prescribed dose), V_{200} (volume when GTV receives 200% of the prescribed dose), and minimum peripheral dose (MPD, the minimum dose re-

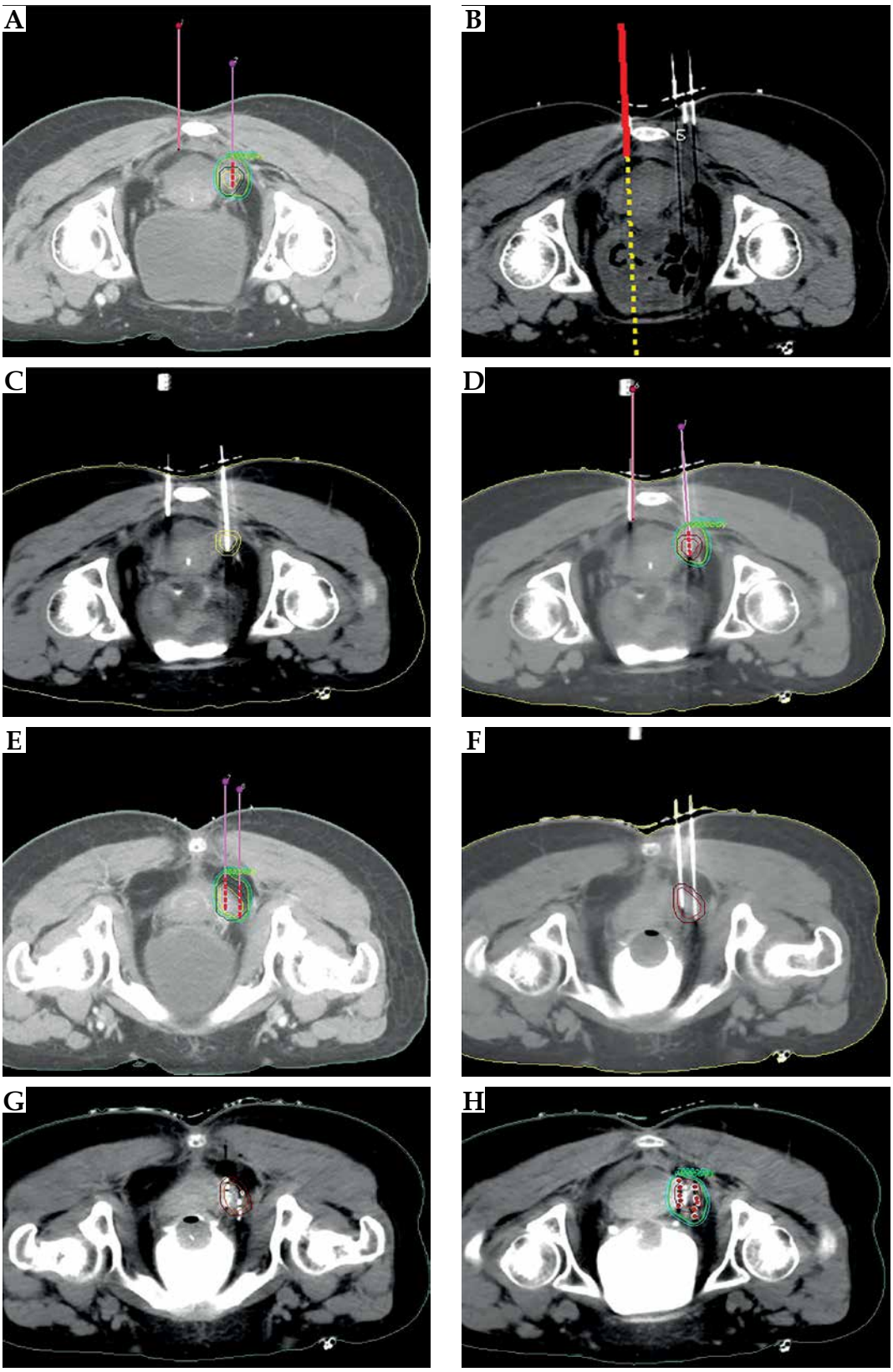

Fig. 2. Flowchart of image navigation system-assisted 3D-printed template-guided radioactive ^{125}I seed implantation. **A**) Pre-operative plan (navigation needle setup); **B**) Navigation-guided insertion of navigation needle; **C**) Seed needles inserted when the navigation needle was in place; **D**) Pre-operative images fused with intra-operative images to measure the errors (angle, insertion point, and tip) of the navigation needle; **E**) Pre-operative plan; **F**) 3D-printed templates and CT-guided seed needles insertion; **G**) Seeds implantation; **H**) Dose verification

ceived at the edge of GTV) in the target area. With regard to conformal index (CI) [10], CI = $(V_{T, ref}/V_T) \times (V_{T, ref}/V_{ref})$, where V_T, $V_{T, ref}$, and V_{ref} are the volume of target area, the volume of target area receiving the prescribed dose, and the total volume (cm^3) contained in the prescribed dose, respectively. The optimal CI was 1, which indicated that the prescribed dose covered the target area, but the received dose outside the target area was lower than the prescribed dose. A larger CI indicated that the volume inside the target area receiving the prescribed dose was larger, whereas the volume outside the target area receiving the prescribed dose was smaller. In terms of external index (EI) [11], EI = $(V_{ref} - V_{T, ref})/V_T \times 100\%$. The optimal EI was 0, which suggested that tissues outside the target area received less than the prescribed dose. A higher EI indicated that the volume of the prescribed dose received outside the target area was larger. Regarding homogeneity index (HI) [11], HI = $(V_{T, ref} - V_{T, 1.5ref})/V_{T, ref} \times 100\%$, where $V_{T, 1.5ref}$ is the volume (cm^3) of the target area receiving 150% of the prescribed dose. The ideal optimal HI was 100%. A higher HI suggested a more uniform dose distribution in the target area. As the location of lesions was scattered and adjacent organs at risk varied, this study was not designed to compare doses of organs at risk.

Other treatment information: In the brachytherapy treatment planning system, other pre-operative and post-operative treatment parameters were collected and compared, including GTV and numbers of needles and seeds.

Table 1. Baseline information of patients and lesions

Characteristic	Number (range)	Proportion (%)
Gender		
Male	17	63.0
Female	10	37.0
Age (years), median	59 (34-84)	
KPS, median	80 (60-90)	
Primary disease		
SCC of nasopharynx/head and neck	9	33.3
Colorectal cancer	6	22.2
Cervical cancer	5	18.5
Esophageal cancer	3	11.1
Lung cancer	2	7.4
Breast cancer	1	3.7
Prostatic cancer	1	3.7
Sarcoma	1	3.7
Position of seed		0.0
Head and neck	13	48.1
Chest wall	1	3.7
Pelvic cavity	11	40.7
Retroperitoneal & paravertebral	2	7.4
Prescription dose (Gy), median	130 (110-160)	
Activity of seed (mCi), median	0.5 (0.4-0.64)	
Number of navigation needles		
1	12	44.4
2	5	18.5
3	10	37.0

Statistical methods

For comparisons between groups, Shapiro-Wilk test was first used to verify whether the data in each group were normally distributed. A p-value > 0.05 indicated that data corresponded to normal distribution. For normally distributed data, a t-test (including paired and independent sample t-tests) was applied for comparison, and t-value was used to describe the test value. For non-normally distributed data, a non-parametric test was adopted for comparison (Wilcoxon test for correlated samples and Mann-Whitney U test for independent samples), and a z-value was used to describe the test value. P-values ≤ 0.05 were considered statistically significant, and statistical software SPSS version 25 (IBM Corp., Armonk, NY, USA) was used for all calculations.

Results

A total of 27 patients were included in the study, and 52 navigation needles were used (mean, 2 ±1 needles). The percentage of patients who relapsed after surgery or external radiotherapy, and who refused surgery or radiotherapy were 81% (22 cases) and 19% (5 cases), respectively. Navigation-assisted 3D templates combined with CT-guided radioactive ^{125}I seed implantation could be successfully completed according to established technical procedures. Table 1 shows the baseline information of patients, target lesions, and pre-operative plans. The pre-operative and intra-operative needle angles ranged from 72.5-111.1° and 73.9-109.9°, respectively, and the absolute value of difference between the two groups was 0.0-1.7°. The pre-operative and intra-operative needle depths ranged from 20.0-110.0 mm and 20.0-118.0 mm, respectively, and the absolute value of difference between the two groups was 0-8.9 mm. Table 2 describes the results of comparison between the two groups. In addition, the range, median, and mean values of the error of needle insertion point for the two groups were 0-3.9 mm, 1.3 mm, and 1.7 ±1.0 mm, respectively, and those of the needle tip were 0-0.9 mm, 2.9 mm, and 3.1 ±1.8 mm, respectively. The range and mean values of the needle depth in the head & neck and chest wall were 20.0-66.0 mm and 34.0 ±11.0 mm, respectively, and those in the retroperitoneal and paravertebral and pelvic parts were 43.0-118.0 mm and 58.0 ±17.0 mm, respectively. The results of Mann-Whitney U test showed that there was a significant difference in the needle depth between the two groups ($p < 0.001$). If divided into two groups by position, errors

of retroperitoneal and paravertebral and pelvic cavity were significantly larger than those of the head and neck and chest wall (Table 3), and differences in the angle, depth, and insertion point were statistically significant ($p < 0.05$). Table 4 summarizes the comparison of dosimetry parameters between pre-operative and post-operative plans. With the exception of MPD, other parameters were similar in both groups, and there was no significant difference ($p > 0.05$). The MPD in the post-operative plan was higher than that in the pre-operative plan (mean, 72.1 Gy and 63.8 Gy, respectively; $p = 0.029$). The actual number of seeds used during the surgery was higher than that planned before the operation (mean, 61.4 and 59.7, respectively, $p = 0.031$). The volume of target area (GTV) in the post-operative plan was larger than that in the pre-operative plan (mean, 41.3 cm^3 and 40.2 cm^3, respectively, $p = 0.005$). In terms of post-operative dose quality evaluation, the results were excellent in 18 cases (67%), good in 6 cases (22%), fair in 2 cases (7%), and poor in 1 patient (4%). Of the 2 patients with fair evaluation quality, one case involved the head and neck, and the other involved the pelvic area, with a post-operative D_{90} of 128.4% (166.9 Gy/130 Gy) and 87.7% (131.5 Gy/150 Gy) of the prescribed dose, respectively. One case with poor evaluation quality was a pelvic case, and the post-operative D_{90} was 79.8% of the prescribed dose (103.7 Gy/130 Gy).

Discussion

Although brachytherapy treatment planning system enables doctors to develop more rational treatment plans before procedure, if the position of seed needle is not accurate during surgery, it is often difficult for post-operative dose to meet the expectations of pre-operative plan, thus affecting follow-up treatment. The ultimate goal of both 3D templates and image navigation system technologies is to allow more accurate insertion of the seed needle according to pre-operative plan. In terms of 3D templates, a number of related studies have described their good accuracy, with post-operative dose meeting the requirements of pre-operative plan [2, 7, 8]. Image navigation systems are another solution for puncture intervention technology. This technology fuses and registers CT, magnetic resonance, or positron emission tomography images obtained before the procedure, with intra-operative real-time images. During the operation, the position of puncture needle is tracked in real-time by a tracer (optical or magnetic positioning) to locate the lesion on the fusion image, thereby guiding the operator to perform the puncture [12]. Owing to their real-time, dynamic, and visible characteristics, image navigation systems are widely used in biopsy, ablation, and other puncture-related procedures [13-15]. However, the combination of the two techniques for radioactive ^{125}I seed implantation and its application in the treatment of tumors of many parts of the body have rarely been reported. Current data show that the accuracy of image navigation system-assisted 3D template-guided radioactive ^{125}I seed implantation treatment is good.

According to different positioning principles, image navigation systems mainly include magnetic and optical positioning and navigation [16]: 1. Magnetic positioning and navigation mainly fix the sensor coil on a tracked

Table 2. Comparison of pre-operative and intra-operative angle and depth of navigation needle –

Parameter	Pre-operative		Intra-operative (actual)		Absolute value of error		Shapiro-Wilk significance (pre-/intra-operative)	Normal distribution	Test value (*z*)	*p*-value (Wilcoxon)
	Median	Mean	Median	Mean	Median	Mean				
Angle (degree)	90	90.8 ±5.5	90.0	90.7 ±5.4	0.4	0.5 ±0.5	< 0.001/ < 0.001	No	–1.1	0.271
Depth (mm)	40.0	43.0 ±18.0	43.0	44.0 ±18.0	3.0	4.0 ±2.0	< 0.001/ < 0.001	No	–3.172	0.002

Table 3. Comparison of navigation needle error between different body parts

Parameter	Head and neck and chest ($n = 14$)			Retroperitoneal and paravertebral and pelvic ($n = 13$)			Shapiro-Wilk significance (HNC/RPP)*	Normal distribution	Test value (*t*/*z*)	*p*-value (independent-*t*/ Mann-Whitney *U*)
	Range	Median	Mean	Range	Median	Mean				
Angle error (degree)	0.0-1.7	0.0	0.4 ±0.6	0.0-1.4	0.5	0.6 ±0.4	< 0.001/ 0.068	No	–2.739	0.006
Depth error (mm)	0.0-6.2	3.0	2.7 ±1.6	0.0-8.9	0.5	0.5 ±0.3	0.041/ 0.172	No	–2.298	0.022
Insertion point error (mm)	0.0-2.6	1.3	1.2 ±0.5	0.0-3.9	2.3	2.2 ±1.2	< 0.001/ 0.073	No	–3.01	0.003
Tip error (mm)	1.5-4.0	2.9	2.7 ±0.8	0.0-8.8	4.0	3.7 ±2.5	0.064/ 0.541	Yes	–1.755	0.092

HNC – head and neck and chest, RPP – retroperitoneal and paravertebral and pelvic

Table 4. Comparison of dosimetry parameters between pre-operative and post-operative plans

Parameter	Pre-operative			Post-operative			Shapiro-Wilk significance (pre-/post-operative)	Normal distribution	Test value (t/z)	p-value (paired-t/ Wilcoxon)
	Range	Median	Mean	Range	Median	Mean				
GTV (cm^3)	10.1-137.1	33.6	40.2 ±28.2	10.3-137.1	33.5	41.3 ±27.9	0.001/0.001	No	–2.813	0.005
Needle	8.0-35.0	13.0	15.2 ±6.5	7.0-35.0	14.0	14.9 ±6.6	0.009/0.010	No	–1.378	0.168
Seed	26-135	54.0	59.7 ±24.2	26.0-135.0	59.0	61.4 ±24.3	0.021/0.012	No	–2.154	0.031
D_{90} (Gy)	109.6-163.7	139.3	141.0 ±15.2	103.7-167.4	145.3	141.9 ±17.1	0.077/0.027	No	–0.762	0.446
MPD (Gy)	23.5-92.4	60.5	63.8 ±20.6	45.2-104.0	71.3	72.1 ±16.7	0.135/0.539	Yes	–2.307	0.029
V_{100} (%)	85.1-99.7	93.2	93.8 ±3.6	87.3-100.0	94.5	94.2 ±3.7	0.128/0.120	Yes	–0.410	0.685
V_{150} (%)	34.5-89.8	69.2	70.4 ±13.1	37.3-94.1	68.2	70.0 ±14.6	0.217/0.508	Yes	0.214	0.832
V_{200} (%)	14.6-77.6	38.5	41.0 ±17.4	18.4-74.1	37.5	41.3 ±15.9	0.037/0.012	No	–0.521	0.603
CI	0.4-0.8	0.60	0.6 ±0.1	0.4-0.9	0.59	0.6 ±0.2	0.094/0.059	Yes	–0.289	0.775
EI (%)	9.0-99.0	31.5	45.6 ±31.2	6.3-152	27.7	47.5 ±37.8	0.001/0.002	No	–0.445	0.657
HI (%)	9.0-61.9	25.9	24.9 ± 12.2	3.4-57.1	28.3	26.3 ±13.6	0.034/0.406	No	–0.747	0.455

device (such as puncture device). When the sensor coil moves relative to the magnetic field emitter, it produces different intensity currents and then, locates the tracked device through current signal. 2. Optical positioning and navigation are primarily used to fix the tracer on the CT machine and tracked device, and infrared camera is used to directly detect the position of tracer. Compared with magnetic positioning, optical positioning is faster in data transmission and has higher accuracy. The disadvantage is that there can be no obstruction between the optical camera and tracked device, and the position of the needle tip cannot be tracked. Optical positioning and navigation were adopted in the present study, but the optical positioning and navigation tracer was large and occupied a large space after being fixed to the seed needle. Furthermore, radioactive ^{125}I seed implantation is a multi-needle operation, so it is impossible to equip all seed needles with tracers. Therefore, in the current research, the main function of navigation was to confirm whether template resetting was accurate. We selected 1-3 navigation needles, and if the position of the navigation needle was accurate, it would prove that the position of the template was accurate, but also the precision of the needle under template guidance was good and subsequent needle insertions could be carried out without navigation. We wanted to know the actual needle track error in patients and its impact on dosimetry distribution.

Based on this study, the needle accuracy under the image navigation system with 3D templates was good. The mean errors of the angle, depth, insertion point, and tip were 0.5 ±0.5°, 4.0 ±2.0 mm, 1.7 ±1.0 mm, and 3.1 ±1.8 mm, respectively. Therefore, the mean error of the angle was < 1°, and the mean error of the distance was approximately 3 mm. Compared with previous studies on 3D templates and/or image navigation system-assisted brachytherapy (the average tip error was 0.86-7.00 mm, and the average angle error was 1.9-5.6°), the accuracy of our study was similar or even better [4, 17-19]. Good accuracy reduces the number of CT scan confirmations and shortens the overall operation time. For angle comparison, the pre-operative and intra-operative angles were not significantly different (p = 0.271), but the intra-operative depth was slightly greater than the pre-operative depth (44.0 ±18.0 mm and 43.0 ±18.0 mm, respectively, p = 0.002). The reasons for the errors were considered to be changes in skin contour and thickness caused by anesthesia, template alignment issues, and unsatisfactory fit between template and body surface. In terms of the treatment site, angle, depth, and insertion point, the errors in the pelvic/retroperitoneal region were larger than those in the head, neck, and chest wall (p < 0.05). In addition, these errors might be attributed to longer insertion paths that led to greater errors (the difference in insertion depth between the two groups was statistically significant, p < 0.05). Moreover, the stability of tissues and organs in the head, neck, and chest wall treatment area was better than that in the pelvic/retroperitoneal region. This prompted us to focus on the accuracy of needle insertion and perform multiple CT scans to confirm if it was necessary in areas where the treatment location was deep, and the tissue was soft and prone to change.

By comparing the pre-operative and post-operative dosimetry parameters in this study, we found that most were not significantly different, suggesting that the post-operative dose could better meet the requirements of pre-operative plan. The only dosimetry index with a significant difference was MPD, which was alternatively expressed as D_{100} (when GTV receives 100% of the dose). MPD in the post-operative plan was higher (p < 0.05), indicating that the error in this study did not result in a reduction in dose to the target area. The reason may be that we replanted seeds in the patients, whose immediate post-operative CT scans showed unsatisfactory seed distribution. This also explains why the number of seeds in the post-operative plan was higher than that in the pre-operative plan, and the difference was statistically significant (p = 0.031). Moreover, GTV in the post-operative plan was larger than that in the pre-operative plan

(p = 0.005), which was possibly related to intra-operative and post-operative bleeding, edema, and inflammatory reactions. The post-operative D_{90} of the three cases with fair and poor evaluation quality did not reach 90% and 80% of the prescribed dose, respectively, suggesting that radioactive ^{125}I seed implantation is a surgery-dependent treatment. Because the dose limit of most normal tissues in the treatment of radioactive ^{125}I seed implantation is not clear, except for rectum and urethra [20], OARs' dose should not exceed the prescribed dose and should be as low as possible in planning design (but there is no specific value to limit), and then the dose data of OARs for analysis could be recorded if necessary. It is believed that the accuracy of treatment would improve, as physicians become more experienced and proficient with the procedure. Many studies have analyzed the dose accuracy of radioactive ^{125}I seed implantation, guided by 3D templates, and results indicate that dose accuracy was good [2, 8, 21, 22]; however, there was no analysis of needle path error in these studies. Due to large volume of navigation tracer and the need for optical tracking, it can only be placed in the body or tail of the seed needle; therefore, it is impossible to navigate all needles. This study is only a preliminary exploration of the feasibility of navigation combined with 3D templates for seed implantation. Until the instruments are improved, and the combination of navigation systems and 3D-templates is further explored, we cannot be confident whether the combined mode is better than the simple application of template.

Based on above analysis, the solutions we propose to reduce errors of implants include the following: 1. While designing the template, areas with significant body surface features should be included for better accuracy and stability of the alignment of 3D template. 2. Moderate kneading after local infiltration anesthesia, which could not only promote the absorption of anesthetics, but also reduce body surface deformation. 3. The shortest needle track should be selected to reduce the influence of deviation in needle insertion. 4. During seed implantation, the force of pull out the needle and push in the seed should be moderate to avoid changes in needle position and seed shifting. 5. The combination of navigator and needle should be improved to realize multi-needle navigation. 6. Immediate post-operative CT allows for real-time observation of seed distribution. For patients with poor seed distribution, timely replanting of seeds could effectively prevent cold spot of the dose in target area [1]. In addition, high-dose-rate (HDR) brachytherapy can often be used as dose compensation for external beam irradiation [23, 24]; similarly, HDR brachytherapy might be considered to compensate implant inaccuracies with post-operative optimization.

The limitations of this study are as follows: 1. The technical development time was slightly short, and the sample size was small. 2. The results were limited to comparisons between treatment plans, and further observation and follow-up are needed. 3. Due to the small number of cases and scattered treatment sites, effective comparison of the dose distribution to different OARs was not available. 4. The combination and process of the image navigation system with 3D templates remain in the initial stages, and need further exploration and improvement. In a follow-up study, we will include more cases and conduct in-depth and detailed research.

Conclusions

The combination of image navigation system and 3D-printed template technologies for radioactive iodine-125 seed implantation treatment showed good accuracy and feasibility, and exhibited good quality regrading completion of implantation plan. Errors in the actual needle insertion during the surgery were smaller than those before the procedure. The actual D_{90} of target area, CI, and dose uniformity, all met the design requirements of the pre-operative plan. In a follow-up study, we will expand the number of cases, refine the study, and clarify the efficacy and safety of this approach based on clinical data.

Financial support/funding

National Key R&D Program of China (2019YFB1311305). Key Clinical Project of Peking University Third Hospital (BYSYZD2019010).

Disclosure

The authors report no conflict of interest.

References

1. Wang J, Chai S, Zheng G et al. Expert consensus statement on computed tomography-guided (125)I radioactive seeds permanent interstitial brachytherapy. *J Cancer Res Ther* 2018; 14: 12-17.
2. Ji Z, Jiang Y, Guo F et al. Dosimetry verification of radioactive seed implantation for malignant tumors assisted by 3D printing individual templates and CT guidance. *Appl Radiat Isotopes* 2017; 124: 68-74.
3. Liu S, Wang H, Wang C et al. Dosimetry verification of 3D-printed individual template based on CT-MRI fusion for radioactive 125I seed implantation in recurrent high-grade gliomas. *J Contemp Brachytherapy* 2019; 11: 235-242.
4. Zhang GH, Lv XM, Wu WJ et al. Evaluation of the accuracy of computer-assisted techniques in the interstitial brachytherapy of the deep regions of the head and neck. *Brachytherapy* 2019; 18: 217-223.
5. Nath R, Anderson LL, Luxton G et al. Dosimetry of interstitial brachytherapy sources: Recommendations of the AAPM Radiation Therapy Committee Task Group No. 43. *Med Phys* 1995; 22: 209-234.
6. Rivard MJ, Coursey BM, DeWerd LA et al. Update of AAPM Task Group No. 43 Report: A revised AAPM protocol for brachytherapy dose calculations. *Med Phys* 2004; 31: 633-674.
7. Wang J, Zhang F, Guo J et al. Expert consensus workshop report: Guideline for three-dimensional printing template-assisted computed tomography-guided (125)I seeds interstitial implantation brachytherapy. *J Cancer Res Ther* 2017; 13: 607-612.
8. Ji Z, Jiang Y, Su L et al. Dosimetry verification of 125I seeds implantation with three-dimensional printing noncoplanar templates and CT guidance for paravertebral/retroperitoneal malignant tumors. *Technol Cancer Res Treat* 2017; 16: 1044-1050.
9. Keyes M, Morris WJ, Spadinger I et al. Radiation oncology and medical physicists quality assurance in British Columbia Cancer Agency Provincial Prostate Brachytherapy Program. *Brachytherapy* 2013; 12: 343-355.

10. van't Riet A, Mak AC, Moerland MA et al. A conformation number to quantify the degree of conformality in brachytherapy and external beam irradiation: application to the prostate. *Int J Radiat Oncol Biol Phys* 1997; 37: 731-736.
11. Saw CB, Suntharalingam N. Quantitative assessment of interstitial implants. *Int J Radiat Oncol Biol Phys* 1991; 20: 135-139.
12. Wood BJ, Kruecker J, Abi-Jaoudeh N et al. Navigation systems for ablation. *J Vasc Interv Radiol* 2010; 21: 257-263.
13. Wu J, Zhou P, Luo X et al. Novel laser positioning navigation to aid puncture during percutaneous nephrolithotomy: a preliminary report. *World J Urol* 2019; 37: 1189-1196.
14. Appelbaum L, Solbiati L, Sosna J et al. Evaluation of an electromagnetic image-fusion navigation system for biopsy of small lesions: assessment of accuracy in an in vivo swine model. *Acad Radiol* 2013; 20: 209-217.
15. Liu FY, Yu XL, Liang P et al. Microwave ablation assisted by a real-time virtual navigation system for hepatocellular carcinoma undetectable by conventional ultrasonography. *Eur J Radiol* 2012; 81: 1455-1459.
16. Ricci WM, Russell TA, Kahler DM et al. A comparison of optical and electromagnetic computer-assisted navigation systems for fluoroscopic targeting. *J Orthop Trauma* 2008; 22: 190-194.
17. Zhou Z, Yang Z, Jiang S et al. Design and validation of a surgical navigation system for brachytherapy based on mixed reality. *Med Phys* 2019; 46: 3709-3718.
18. Mehrtash A, Damato A, Pernelle G et al. EM-navigated catheter placement for gynecologic brachytherapy: an accuracy study. *Proc SPIE Int Soc Opt Eng* 2014; 9036: 90361F.
19. Huang MW, Zhang JG, Zheng L et al. Accuracy evaluation of a 3D-printed individual template for needle guidance in head and neck brachytherapy. *J Radiat Res* 2016; 57: 662-667.
20. Zaorsky NG, Davis BJ, Nguyen PL et al. The evolution of brachytherapy for prostate cancer. *Nat Rev Urol* 2017; 14: 415-439.
21. Zhang H, Dev D, Yu H et al. Feasibility of three-dimensional-printed template-guided (125)I seed brachytherapy and dosimetric evaluation in patients with malignant tumor. *J Cancer Res Ther* 2019; 15: 793-800.
22. Chen Y, Jiang Y, Ji Z et al. Dosimetry, efficacy, and safety of three-dimensional printing noncoplanar template-assisted and CT-guided (125)I seed implantation for recurrent retroperitoneal lymphatic metastasis after external beam radiotherapy. *Brachytherapy* 2020; 19: 380-388.
23. Shahid N, Loblaw A, Chung HT et al. Long-term toxicity and health-related quality of life after single-fraction high dose rate brachytherapy boost and hypofractionated external beam radiotherapy for intermediate-risk prostate cancer. *Clin Oncol (R Coll Radiol)* 2017; 29: 412-420.
24. Okuma K, Yamashita H, Kobayashi R et al. A study of high-dose-rate intracavitary brachytherapy boost for curative treatment of uterine cervical cancer. *J Contemp Brachytherapy* 2015; 7: 128-134.